

# Effects of contour propagation and background corrections in different MRI flow software packages

D Boye<sup>1</sup>, O Springer<sup>2</sup>, F Wassmer<sup>3</sup>, S Scheidegger<sup>3</sup>,  
L Remonda<sup>1</sup> and J Berberat<sup>1</sup>

Acta Radiologica Open

4(6) 1–6

© The Foundation Acta Radiologica  
2015

Reprints and permissions:

[sagepub.co.uk/journalsPermissions.nav](http://sagepub.co.uk/journalsPermissions.nav)

DOI: 10.1177/2058460115589124

[arr.sagepub.com](http://arr.sagepub.com)



## Abstract

**Background:** Velocity-encoded magnetic resonance imaging (VENC-MRI) is a commonly used technique in cardiac examinations. This technique utilizes the phase shift properties of protons moving along a magnetic field gradient. VENC-MRI offers a unique way of measuring the severity of valve regurgitation by directly quantifying the regurgitation flow volume.

**Purpose:** To compare flow analysis results of different software programs and to assess the effect of background correction in sample patient cases.

**Material and Methods:** A phantom was built out of Polymethyl methacrylate (PMMA) which provides tubes of different diameters. These tubes can be connected to an external water circuit to generate a water flow inside the tubes. Expected absolute flow quantities inside the tubes were determined from preset tube- and flow-parameters. Different flow conditions were measured with a VENC-MRI sequence and the images evaluated using different software packages. In a second step six randomly selected patients showing different degrees of aortic insufficiency were evaluated in clinical terms.

**Results:** The contour propagation algorithms used in the software packages performed differently even on static phantom geometry. In terms of clinical evaluation the software packages performed similarly. Enabling background correction or leaving out manual correction of propagated contours changed results for severity of aortic insufficiency.

**Conclusion:** Turning on background correction and manual correction of propagated contours in MRI flow volume measurements is strongly recommended.

## Keywords

Magnetic resonance imaging (MRI) flow, cardiac MR (CMR), software comparison, aortic insufficiency

Date received: 9 December 2014; accepted: 7 May 2015

## Introduction

Velocity-encoded magnetic resonance imaging (VENC-MRI) is a commonly used technique in cardiac examinations (1,2). There is also growing interest for using this technique in brain examinations (3,4).

VENC-MRI utilizes the phase properties of protons moving parallel to a magnetic field gradient. These protons undergo a phase shift which is proportional to their velocity. Subtracting a reference scan from a velocity encoded scan results in phase contrast velocity maps. Clinical applications of VENC-MRI include measurement of valve regurgitation severity (5–7) or detection of hemodynamic significance of stenosis (8).

For patients with valve regurgitation VENC-MRI is a unique technique compared to other imaging

modalities as it can directly quantify the regurgitation in mL/min (9). A device used to directly quantify a physical property needs quality assurance (QA). Summers et al. (10) presented a phantom for flow measurement and assessed it in a multisite trial. Their phantom consists of straight, stenosed, and U-bend flow

<sup>1</sup>Cantonal Hospital Aarau, Department of Neuroradiology, Aarau, Switzerland

<sup>2</sup>Cantonal Hospital Aarau, Department of Radiology, Aarau, Switzerland

<sup>3</sup>Zurich University of Applied Sciences, Institute of Applied Mathematics and Physics, Winterthur, Switzerland

### Corresponding author:

Jatta Berberat, Kantonsspital Aarau, Tellstrasse 25. CH-5001 Aarau, Switzerland.

Email: [jatta.berberat@ksa.ch](mailto:jatta.berberat@ksa.ch)



channels embedded in polymer layers. These static agarose layers can be used for background offset correction.

Inter-study reproducibility of VENC-MRI was assessed and the variability was found to be very low (11). One of the major reasons for errors in velocity encoded measurements is the existence of field inhomogeneities inside the scanner. These lead to eddy current effects which will in turn introduce spatially dependent phase distortions (12). These distortions or phase offsets can be corrected by analyzing areas with static tissue to derive a correction function for the offset error (12,13). Phase errors caused by concomitant fields (14) are corrected during postprocessing as implemented in the scanner software.

To analyze flow through a specific region of VENC-MRI images a region of interest has to be delineated. In case of patients with aortic insufficiency images of a two-dimensional (2D) slice perpendicular to the aorta are acquired at multiple time frames throughout the R-R interval of the heart cycle. As the cross-section and the position of the aorta changes over time the region of interest (ROI) has to be adjusted for all time frames. Van der Geest et al. (15) presented an automatic contour propagation algorithm where only the center of the aorta on one time-frame needs to be selected by the user. Automatic propagation could be done in about 6 s compared to 10 min of manual contouring.

Inter- and intra-observer variabilities for manual and automatic detection of the aortic contour was shown to be low demonstrating that the automatically detected contours detection yielded reproducible results (15). Misalignments of contours by errors in propagation algorithms present an additional source of errors for VENC-MRI measurements.

The aim of this study was to compare flow analysis results of different software programs and to assess the effect of background correction and contour misalignment for sample patient cases. Comparison results should show the impact of the assessed effects and from that give a guideline for necessary steps in the physician's workflow.

## Material and Methods

### Phantom

The phantom consists of a cylinder out of Polymethylmethacrylate (PMMA) with a diameter of 300 mm. By filling the phantom with distilled water a signal for phase offset calculations is provided. Six tubes showing different flow configurations (e.g. constant tube diameter or varying tube diameter to simulate different degrees of stenosis) were placed inside the phantom. The diameters of the inner tubes were 24 mm and

10 mm with several possible stenosis lengths. A seventh tube inside the phantom allows for inserting smaller tubes with customized flow configurations. Fig. 1 shows a three-dimensional (3D) model of the phantom.

A water circuit was designed to enable continuous measurements of different flow rates (Fig. 2). To allow for simple changes and direct control of flow rates the pump was placed outside of the MRI room. A frequency converter was used to change flow rates of the water pump. The flow rates were measured by rotameters directly behind the pump for comparison to the MRI measurements.

Expected mean flow velocity inside the tube was calculated with following formula:

$$v = \frac{4f}{\pi d^2} \quad (1)$$

where  $v$  is the expected velocity,  $f$  the flow rate, and  $d$  the tube diameter.

### Software

Four different commercially available software packages and manual postprocessing done in MATLAB (The MathWorks Inc., Natick, MA, USA) were compared. The software packages used were Siemens Argus Flow (Siemens Healthcare, Erlangen, Germany (16)), circle CVI42 (Circle Cardiovascular Imaging Inc., Calgary, Canada (17)), Medviso Segment (Medviso AB, Lund, Sweden (18)), and Medis Q-Flow (Medis Medical Imaging Systems BV, Leiden, The Netherlands (19)).

### Patients

Six patients were selected to cover regurgitation fraction in the range of 0–40%. The age of selected patients was in the range of 21–72 years (5 women, 1 man).

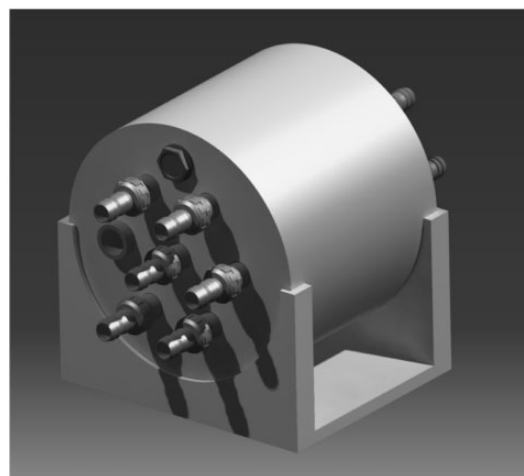
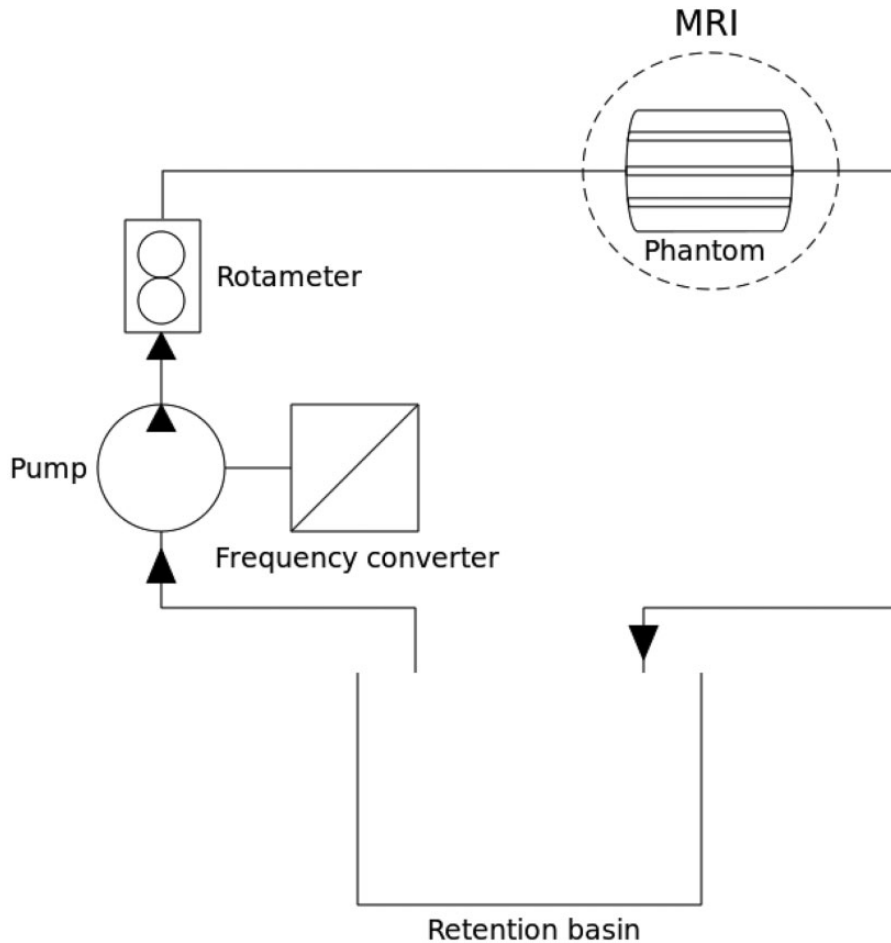


Fig. 1. 3D model of the phantom.



**Fig. 2.** Flow circuit set-up.

### *Image acquisition*

Images were acquired on an Avanto 1.5T and on a Skyra 3T (Siemens Healthcare) using Siemens' standard VENC encoded flow sequence "FLASH". For the phantom measurements an ECG curve was simulated and used to acquire eight time-frames with a TR of 117ms, a TE of 3.34ms, a flip angle of 20 degrees, a slice thickness of 6mm, and an in-plane resolution of 0.9mm. Patient's R-R intervals were acquired in 30 time-frames using the same sequence with enabled ECG triggering, a TR of 39.76ms, a TE of 2.68ms, a flip angle of 20 degrees, a slice thickness of 6mm, and an in-plane resolution of 1.77mm.

### *Software operating procedure*

The operating procedure for the phantom was to delineate the tube on the first time-frame, then run the contour propagation algorithm to create delineations on all succeeding time-frames. No manual correction was applied afterwards.

For patient cases, contours were manually corrected if needed. Resulting forward and backward flow volumes were collected for original automatic contours and for manually corrected ones to inspect differences. Additionally also background corrected values were calculated for both cases. All software packages support "static tissue background correction" so this correction was applied in all cases. A region inside the back muscles of each patient was selected as static-tissue region. As there is no contour propagation involved in the background correction calculation the same correction values were applied in all software packages.

Manual postprocessing in MATLAB was done for the phantom measurements by selecting the ROI pixel-by-pixel on magnitude images.

## **Results**

### *Phantom*

The results for the phantom measurements are shown in Table 1. The average absolute deviation for detected area and mean flow velocity were below 2% for CVI42,

**Table 1.** Mean flow velocity and area results for phantom measurements.

Flow (cm/s)	Area (mm <sup>2</sup> )	Argus deviation (%)		CVI42 deviation (%)		Segment deviation (%)		Q-Flow deviation (%)		MATLAB deviation (%)	
		Flow	Area	Flow	Area	Flow	Area	Flow	Area	Flow	Area
20.0	452.4	-3.0	+4.9	+1.2	-1.6	+2.1	-3.4	-1.7	+4.0	-0.2	+1.3
50.0	452.4	-7.1	+9.6	-1.8	+0.4	-1.1	-1.0	-4.2	+6.0	-1.9	+1.3
100.0	452.4	-0.3	+5.1	+2.0	+3.3	+3.8	-0.8	+0.9	+5.9	+3.2	+1.3
42.4	78.5	-2.2	-8.4	-1.5	-2.3	-2.4	+0.3	-14.6	+18.9	-2.5	-0.9
63.6	78.5	-0.5	-2.7	+0.6	+0.5	+0.5	+2.2	-10.0	+21.3	+1.0	-0.9
106.1	78.5	+0.9	-5.3	+0.9	+1.3	+1.2	+1.8	-8.0	+22.4	+1.5	-0.9
169.7	78.5	-3.0	-0.9	-0.8	+1.2	-0.9	+3.2	-7.9	+20.3	-0.3	-0.9
Average deviation		-2.2	+0.3	+0.1	+0.4	+0.5	+0.3	-6.5	+14.1	+0.1	+0.1
Avg. absolute dev.		2.5	5.3	1.3	1.5	1.7	1.8	6.8	14.1	1.5	1.1

Segment and manual masking in MATLAB. Contour propagation in Argus resulted in a too large area for the tube with a diameter of 24 mm (area = 452.4 mm<sup>2</sup>) and in a too small area for the tube with a diameter of 10 mm (area = 78.5 mm<sup>2</sup>). Average absolute deviation in Argus for the area was 5.3% and for the mean flow velocity 2.5%. Q-Flow's contour propagation estimated a too large area for both tube sizes resulting in an average absolute deviation for flow and area of 6.8% and 14.1%, respectively.

### Software

Table 2 shows the different features available for simple flow measurements in each of the software packages. Some software manufacturers provide other features like T1, T2/T2\* Mapping, tissue characterization, perfusion, 4D viewing, etc. together with VENC analysis or in additional software packages. Here only the part for VENC analysis of each software package was tested so additional features were not listed in Table 2.

### Patients

After manual correction of contours all software packages showed similar results in regurgitant fraction for patient measurements (Table 3). Leaving out manual correction of propagated contours showed a maximum difference of 6.6% for Patient P3 using CVI42.

Highest difference for enabling background correction of 7.2% was found using Q-Flow for patient P1. Mean velocity offset was -2.5 cm/s with a maximum velocity of 96 cm/s in this case.

### Discussion

In clinical day-to-day routine of analyzing aortic flow, physicians contour the aorta on one time-

frame where the aorta is clearly visible and let the software propagate this first contour onto all cardiac phases. In a second step, contours are typically corrected manually. For clinical evaluation the quota of backward flow volume to forward flow volume (regurgitant fraction) is analyzed. According to this clinical procedure six patient cases were compared by first delineating the aorta where it showed well visible borders. Then the contour propagation was run and afterwards the contours were manually corrected if needed.

For the phantom measurements CVI42 and Segment showed best agreement in terms of detected area and mean velocity inside the tubes. Using MATLAB to manually mask the tubes in the images yielded similar results. No manual correction was applied afterwards as the goal was to test the detection of a simple clearly delimited circular geometry.

Q-Flow showed the worst results for the phantom measurements but this could be due to some part of the algorithm which does not affect clinical evaluation. The exact functional principle of the algorithm is unknown at this point but it is important to note that there are such large differences in contour propagation. In response to an inquiry by email Medis (Medis Medical Imaging Systems BV, Leiden, The Netherlands (19)) pointed out that the contour detection was revised in their new Version 5.6 which our institute was not yet upgraded to.

Comparison of patient evaluation showed that the effect of background correction is non-neglectable. Gatehouse et al. (20) showed that a velocity offset correction of 2.4 cm/s could result in up to a 10% difference in regurgitant fraction. They also proposed that the maximum offset which does not need correction is 0.6 cm/s. Mean offset error was 2.7% for their multi-site phantom based study. These results are in agreement with the results presented in this paper where a

**Table 2.** Available features in software programs used for this study.

	Argus	CVI42	Segment	Q-Flow
Contour propagation	x	x	x	x
2D flow velocity profile		x	x	x
3D flow velocity profile			x	
ROI BG correction	x	x	x	x
Surrounding contour BG correction				x
Phantom BG correction		x	x	
Polynomial fit BG correction			x	
Static tissue BG correction			x	x
Distance measurement	*	x	x	x
Play movie	X	x	x	x
Save movie	X	x	x	
License	Commercial†	Commercial	Free non-commercial, commercial	Commercial

\*Available in standard viewer of Siemens system but not in the Argus window.

†No stand-alone, only available for a Siemens Multimodality Workplace or for a Siemens MR.

BG, background; ROI, region of interest.

mean velocity offset of  $-2.5$  cm/s showed a difference in regurgitant fraction of 7.2%.

One limitation of the study presented here was the estimation of phase offset due to magnetic field inhomogeneities by deriving a linear correction function from areas containing static tissue (12–14). This first approximation of background offset was chosen as this type of correction is supported by all compared software packages. To use phantom calibration measurements is a more precise method for background correction (21) but doubles measurement time and is not done in the clinical routine of our institute (see Table 1 for software packages which provide phantom offset correction).

Giese et al. (22) presented an alternative approach to use magnetic field monitoring to calculate background velocity offset corrections. They showed that echo times can be optimized to minimize background offset and by additionally using the calculated offsets, the errors could be decreased to less than 0.5%. This is a promising method for background correction as it is very accurate and does not lengthen measurement time.

A second limitation is the size of the patient set. The purpose of this study was not to show statistically significant differences in contour propagation but to confirm that manual contour correction should be done by default and to show that background offset correction has an impact on clinical evaluation of patients. Ignoring errors of automatically propagated contours lead to differences in regurgitant fraction of the same dimension as the ones resulting from background offset. This could mislead the clinical evaluation of the severity of aortic insufficiency.

**Table 3.** Regurgitant fraction in % representing the severity of aortic insufficiency.

Patient	Backward forward flow volume quota (severity)/same with manually corrected contours (%)			
	Argus	CVI42	Segment	Q-Flow
P1	33.9/30.2	32.0/32.0	32.0/32.0	34.3/32.6
P1_BGC	27.5/24.4	25.7/25.7	25.7/25.7	27.1/25.5
P2	0.0/0.0	0.3/0.3	0.4/0.4	0.6/0.6
P2_BGC	0.0/0.0	0.4/0.4	0.5/0.5	0.8/0.8
P3	10.9/10.9	17.1/10.5	10.9/10.8	11.5/11.6
P3_BGC	16.4/16.4	21.8/15.8	16.6/16.5	17.6/17.7
P4	47.1/47.1	46.6/46.5	46.7/46.7	47.8 /47.7
P4_BGC	40.7/40.7	40.0/40.0	40.0/40.0	40.8/40.7
P5	0.1/0.1	0.1/0.1	0.1/0.1	0.1/0.1
P5_BGC	1.0/1.0	2.7/2.4	2.5/2.5	3.2/3.2
P6	6.5/6.5	8.3/8.3	8.0/8.0	9.8/10.5
P6_BGC	8.9/8.9	10.6/10.6	10.3/10.3	12.4/13.1

BGC, with background correction.

The software package Segment being freely available for research purposes showed reproducible results and provides the highest number of features for flow evaluation. Segment provided all commonly used background correction methods.

In conclusion, contour propagation algorithms showed differences between software programs. Even for a simple static phantom geometry differences in contour detection were seen. For patient cases the contour propagations varied between patients and between

programs. Automatic contour propagation has to be checked and corrected manually if there is a visible discrepancy. In terms of clinical evaluation of regurgitant fraction the different software programs performed similarly.

Enabling background correction or leaving out manual correction of propagated contours lead to non-neglectable changes in regurgitant fraction. Therefore turning on background correction and checking automatically propagated contours for validity is recommended for all MRI flow volume measurements.

### Acknowledgements

The authors thank Kieran O'Brien for his insight into flow encoded MR sequences.

### Conflict of interest

None declared.

### References

1. Gatehouse PD, Keegan J, Crowe LA, et al. Applications of phase-contrast flow and velocity imaging in cardiovascular MRI. *Eur Radiol* 2005;15:2172–2184.
2. Søndergaard L, Lindvig K, Hildebrandt P, et al. Quantification of aortic regurgitation by magnetic resonance velocity mapping. *Am Heart J* 1993;125:1081–1090.
3. Wentland AL, Wieben O, Korosec FR, et al. Accuracy and reproducibility of phase-contrast MR imaging measurements for CSF flow. *Am J Neuroradiol* 2010;31:1331–1336.
4. Levy LM, Chiro GD. MR phase imaging and cerebrospinal fluid flow in the head and spine. *Neuroradiology* 1990;32:399–406.
5. Rebergen SA, Chin JG, Ottenkamp J, et al. Pulmonary regurgitation in the late postoperative follow-up of tetralogy of Fallot. Volumetric quantitation by nuclear magnetic resonance velocity mapping. *Circulation* 1993;88:2257–2266.
6. Rebergen SA, van der Wall EE, Doornbos J, et al. Magnetic resonance measurement of velocity and flow: Technique, validation, and cardiovascular applications. *Am Heart J* 1993;126:1439–1456.
7. Gelfand EV, Hughes S, Hauser TH, et al. Severity of mitral and aortic regurgitation as assessed by cardiovascular magnetic resonance: optimizing correlation with Doppler echocardiography. *J Cardiovasc Magn Reson* 2006;8:503–507.
8. Westenberg JJM, Geest RJ, van der Wasser MNJM, et al. Stenosis quantification from post-stenotic signal loss in phase-contrast MRA datasets of flow phantoms and renal arteries. *Int J Card Imaging* 1999;15:483–493.
9. Hundley WG, Bluemke DA, Finn JP, et al. ACCF/ACR/AHA/NASCI/SCMR 2010 Expert Consensus Document on Cardiovascular Magnetic Resonance - A Report of the American College of Cardiology Foundation Task Force on Expert Consensus Documents. *J Am Coll Cardiol* 2010;55:2614–2662.
10. Summers PE, Holdsworth DW, Nikolov HN, et al. Multisite trial of MR flow measurement: Phantom and protocol design. *J Magn Reson Imaging* 2005;21:620–631.
11. Dulce MC, Mostbeck GH, O'Sullivan M, et al. Severity of aortic regurgitation: interstudy reproducibility of measurements with velocity-encoded cine MR imaging. *Radiology* 1992;185:235–240.
12. Walker PG, Cranney GB, Scheidegger MB, et al. Semiautomated method for noise reduction and background phase error correction in MR phase velocity data. *J Magn Reson Imaging* 1993;3:521–530.
13. Lankhaar J-W, Hofman MBM, Marcus JT, et al. Correction of phase offset errors in main pulmonary artery flow quantification. *J Magn Reson Imaging* 2005;22:73–79.
14. Bernstein MA, Zhou XJ, Polzin JA, et al. Concomitant gradient terms in phase contrast MR: analysis and correction. *Magn Reson Med* 2008;39:300–308.
15. Van der Geest R, Niezen R, van der Wall E, et al. Automated measurement of volume flow in the ascending aorta using MR velocity maps: evaluation of inter- and intraobserver variability in healthy volunteers. *J Comput Assist Tomogr* 1998;22:904–911.
16. Siemens Argus Flow. Available at: <https://www.healthcare.siemens.com/magnetic-resonance-imaging/options-and-upgrades/clinical-applications/argus-flow> (accessed 26 June 2014).
17. circle CVI42. Available at: <https://www.circlecvi.com/features/flow.php> (accessed 26 June 2014).
18. Heiberg E, Sjögren J, Ugander M, et al. Design and validation of Segment - freely available software for cardiovascular image analysis. *BMC Med Imaging* 2010;10:1.
19. Medis Q-Flow. Available at: <http://www.medis.nl/products/qflow.html> (accessed 26 June 2014).
20. Gatehouse PD, Rolf MP, Graves MJ, et al. Flow measurement by cardiovascular magnetic resonance: a multi-centre multi-vendor study of background phase offset errors that can compromise the accuracy of derived regurgitant or shunt flow measurements. *J Cardiovasc Magn Reson* 2010;12:5.
21. Chernobelsky A, Shubayev O, Comeau CR, et al. Baseline correction of phase contrast images improves quantification of blood flow in the great vessels. *J Cardiovasc Magn Reson* 2007;9:681–685.
22. Giese D, Haeberlin M, Barmet C, et al. Analysis and correction of background velocity offsets in phase-contrast flow measurements using magnetic field monitoring. *Magn Reson Med* 2012;67:1294–1302.